Accepted Manuscript

Title: Selective CO removal over Au/CeFe and CeCu catalysts in microreactors studied through kinetic analysis and CFD simulations

Authors: G. Arzamendi, I. Uriz, P.M. Diéguez, O.H. Laguna, W.Y. Hernández, A. Álvarez, M.A. Centeno, J.A. Odriozola, M. Montes, L.M. Gandía

PII: S1385-8947(10)00975-7
DOI: doi:10.1016/j.cej.2010.08.083
Reference: CEJ 7389

To appear in: *Chemical Engineering Journal*

Received date: 28-2-2010
Revised date: 25-8-2010
Accepted date: 30-8-2010

Please cite this article as: G. Arzamendi, I. Uriz, P.M. Diéguez, O.H. Laguna, W.Y. Hernández, A. Álvarez, M.A. Centeno, J.A. Odriozola, M. Montes, L.M. Gandía, Selective CO removal over Au/CeFe and CeCu catalysts in microreactors studied through kinetic analysis and CFD simulations, *Chemical Engineering Journal* (2010), doi:10.1016/j.cej.2010.08.083

Selective CO removal over Au/CeFe and CeCu catalysts in microreactors studied through kinetic analysis and CFD simulations

G. Arzamendi [a], I. Uriz [a], P.M. Diéguez [a], O.H. Laguna [b], W.Y. Hernández [b], A. Álvarez [b], M.A. Centeno [b], J.A. Odriozola [b], M. Montes [c], L.M. Gandía [a,*]

[a] *Departamento de Química Aplicada, Edificio de los Acebos, Universidad Pública de Navarra, Campus de Arrosadía s/n, E-31006 Pamplona, Spain*

[b] *Instituto de Ciencia de Materiales de Sevilla, Centro Mixto CSIC-Universidad de Sevilla, Avda. Américo Vespucio 49, 41092 Sevilla, Spain*

[c] *Departamento de Química Aplicada, Facultad de Ciencias Químicas de San Sebastián, Universidad del País Vasco, Pº Manuel de Lardizábal 3, E-20018, San Sebastián, Spain*

[*] Corresponding author. Phone: +34-948-169605. Fax: +34-948-169606.

E-mail address: lgandia@unavarra.es (L.M. Gandía)

Abstract

A kinetic study of the preferential oxidation of CO in H_2 rich streams (CO-PrOx) over a cerium-copper oxide (CeCu) and a gold catalyst supported on cerium-iron oxide (Au/CeFe) is presented. The gold catalyst is very active but the CeCu oxide is more selective. A kinetic model describing the CO-PrOx system with CO_2 and H_2O in the feed has been formulated considering the oxidation of CO and H_2 and the reverse water-gas shift reaction. The rate equations have been implemented in computational fluid dynamics codes to study the influence of the operating variables on the CO-PrOx in microchannels and microslits. The CeCu catalyst is the only one capable of achieving final CO contents below 10-100 ppmv. Due to the opposite effect of temperature on activity and selectivity there is an optimal

temperature at which the CO content is minimal over CeCu. This temperature varies between 170 and 200 ºC as the GHSV increases from 10 000 to 50 000 h^{-1}. Simulations have evidenced the very good heat transfer performance of the microdevices showing that the CO-PrOx temperature can be controlled using air as cooling fluid although the inlet temperature and flow rate should be carefully controlled to avoid reaction extinction. Both microchannels and microslits behaved similarly. The fact that the microslits are much easier to fabricate may be an interesting advantage in favor of that geometry in this case.

Keywords: CO preferential oxidation (PrOx); Computational fluid dynamics (CFD); Microchannel reactor; Microreactor; Process intensification.

1. Introduction

Low-temperature polymer-electrolyte-membrane fuel cells (PEMFC) require high-purity hydrogen as fuel. Specially, the CO content of the feed should be limited to 10 or 100 ppm, depending on the anode composition. When hydrogen is produced from the reforming of hydrocarbons, alcohols or ethers the CO content in the gaseous stream leaving the water-gas shift unit may vary between *ca.* 0.5 and 2 vol.%, thus CO removal to a trace-level is required. Preferential CO oxidation (CO-PrOx) is among the preferred technologies for small-scale fuel processor applications [1]. Other alternatives such as pressure swing adsorption and separation with membranes require expensive compressors which are difficult to integrate in compact systems. Selective catalytic methanation of CO is very promising but the relatively high temperatures required favor competing side reactions as CO_2 methanation and the reverse water-gas shift (r-WGS). In contrast, the PrOx reaction is carried out inexpensively at atmospheric pressure although carefully measured amounts of air have to be added to the

reformate stream. Improving the selectivity by operating at low temperatures and limiting the r-WGS reaction are the major drivers of CO-PrOx [2,3].

In the case of PEMFCs for portable and automotive applications one of the most important challenges is the availability of compact, light and integrated hydrogen supply systems. Microreactors can help to meet those requirements [4,5]. More specifically, due to the very fast chemical kinetics and exothermicity of CO-PrOx, using microreactors allows avoiding mass and heat transport limitations which results in improved reactor performance and reaction selectivity [6-8]. As reviewed by Ouyang and Besser [8], there are several examples of integrated fuel processors in the power range between 2.4 W_e and 2 kW_e including CO-PrOx units based on microreaction technology. More recently, Kolb et al. [9] and O'Connell et al. [10] have reported on microstructured reactors in the 2.5–5 kW electrical output developed for CO-PrOx reaction although the catalyst used (Johnson Matthey Fuel Cells) was not specified. The PrOx microreactor reduced the CO content from 1 vol.% in the feed to 25-60 ppm at the reactor outlet depending on the fuel cell load level. Dudfield et al. [11,12] operated a compact CO-PrOx reactor containing 2.5% Pt-Ru on hopcalite catalyst designed for 20 kW_e PEMFC applications. The unit allowed reductions in the CO concentrations from 2.7% to less than 20 ppm within a temperature range of 130–200 ºC. Other examples of CO-PrOx in catalyst coated microstructured reactors include the use of several noble metal-based catalysts [13]. A hydrogen-rich stream containing 1.12 vol.% CO and O_2/CO molar ratio of 4 was fed into a microreactor coated with Pt-Rh/γ-Al_2O_3 at gas hourly space velocity (GHSV) of 15 500 h^{-1} resulting in less than 10 ppm of CO in the off-gas at 140–160 ºC. Hwang et al. [14] fabricated a silicon-based microreactor consisting of microchannels coated with a commercial 5 wt.% Pt/Al_2O_3 catalyst. Under optimized conditions this device yielded 99.4% CO conversion and 44.1% selectivity at 260 ºC for a

stream containing 1 vol.% CO and O_2/CO molar ratio of 2 at the very high GHSV of 217 390 h^{-1}.

As can be deduced from the preceding revision much work on CO-PrOx in microreactors has been carried out with catalysts based on noble metals, mainly Pt and Pt combined with Rh and Ru. Nevertheless, Snytnikov et al. [15] used a reactor with microchannels coated with a 5 wt.% Cu/CeO_{2-x} catalyst allowing to reduce the CO concentration from 1 vol.% to 10 ppm at 190 ºC with a selectivity of 60 % and space velocity of 55 000 $cm^3 \cdot g^{-1} \cdot h^{-1}$.

In this work we report on the CO-PrOx reaction over cerium-copper oxide and a new active gold catalyst supported on cerium-iron oxide. The kinetic equations over these catalysts in powder form are first derived from data obtained in a micro packed-bed reactor and then implemented in a computational fluid dynamics (CFD) code to investigate by computer simulation the potential of the catalysts for CO-PrOx intensification in microreactors.

2. Experimental

2.1. Catalysts preparation

The cerium-copper oxide (CeCu, 10 wt.% CuO) was prepared by coprecipitation. The volumes of aqueous solutions (0.5 M) of the nitrates required to get a $Ce(OH)_3$/$Cu(OH)_2$ weight ratio of 9/1 were mixed under vigorous stirring. Then a NaOH solution (2 M) was added dropwise over the metallic mixture until a stable pH of 9 was achieved. The precipitate was separated and washed with distilled water in order to remove sodium and nitrate ions. The resulting solid was dried overnight at 60 °C and finally calcined at 300 ºC for 2 h.

The cerium-iron mixed oxide (CeFe, 10 mol% Fe) was synthesized by a pseudo sol-gel method involving the thermal decomposition (500 ºC, 2 h) of the metallic propionates obtained after dissolution of the adequate amounts of Ce (III) acetate and Fe (III) acetyl

acetonate in propionic acid (0.12 M) [16]. Gold (1 wt.%) deposition over the CeFe oxide was carried out by deposition-precipitation at 70 ºC and pH of 8 using chloroauric acid as the gold source. The resulting solid was washed with deionized water until absence of chloride ion, dried overnight at 60 °C, and finally calcined at 300 ºC for 2 h to yield the Au/CeFe catalyst.

2.2. Kinetic study

The CO-PrOx reaction was carried out at atmospheric pressure in a PID Eng&Tech Microactivity set-up, employing a stainless steel tubular reactor with internal diameter of 9 mm and a constant feedstream flowrate of 100 cm^3/min (STP). The catalyst (100 mg, particle size in the 100–200 μm range) was diluted with crushed glass particles in the same particle size range forming a bed of about 5 mm in length. Two series of experimental runs were carried out to perform the kinetic study. In the first one, the feedstream was composed of 50 vol.% H_2, and the CO and O_2 concentrations were varied within the 0.25–2 vol.% and 0.5–3 vol.% ranges, respectively, using N_2 as balance. To study the effect of CO_2 and H_2O, in the second series of experiments the H_2 content of the feedstream was set at 50 vol.%, and both the CO and O_2 concentrations were fixed at 1 vol.%. The CO_2 and H_2O concentrations in the feed were varied within the 2–10 vol.% and 0–20 vol.% ranges, respectively, using N_2 as balance. The reaction temperature was increased from 50–60 to 190–250 ºC in steps of 10 ºC. For each step the temperature was stabilized and data were recorded at steady-state conditions. Fresh catalyst was loaded into the reactor after each complete run. Some experiments carried out at the same space-time but at varying gas linear velocities confirmed the absence of external mass transfer effects. On-line analyses of the feed and products streams were performed on an Agilent 7890 gas chromatograph equipped with a Porapak Q, two Molecular Sieve 5A and two Hayesep Q columns and two TCD detectors and a FID detector. In general, the conversion and selectivity results were reproducible within 5%.

3. Microreactor models and simulation conditions

Three-dimensional simulations have been carried out using ANSYS CFX software which is based on the finite-volume method for spatial discretization of the Navier-Stokes equations. This code has provided satisfactory results for a variety of microfluidic problems [17-20]. Simulations were performed on a Dell Precision PWS690 workstation running MS Windows XP® × 64 with an available RAM of 16.0 GB.

A first model consisting of square parallel microchannels of 20 mm of length and 0.70 mm of side was developed to study the influence of the operating variables (Fig. 1A). This geometry has been used previously to study the steam reforming of methane and methanol and is described in detail elsewhere [18,19]. In addition, a geometry consisting of parallel microslits of 16 mm width, 0.70 mm depth and 20 mm long was created to be compared with the square microchannels and study possible effects associated to the aspect ratio (Fig. 1B). These models have three main physical domains, two of them are fluidic and the other corresponds to the solid block (stainless steel). These domains were meshed using prismatic and hexahedral elements resulting in dense computational unstructured grids. In order to resolve the boundary layers accurately a mixed unstructured grid approach [21] was applied in the fluidic domain near the solid walls.

CFD simulations have been conducted under stationary conditions. It has been assumed that a thin layer of the CeCu or the Au/CeFe catalysts was uniformly deposited onto the walls of the microreactors at loadings of 1, 2 and 5 mg/cm^2. The feedstream composition was set at 70 vol.% H_2, 1 vol.% CO, 10 vol.% CO_2 and 10 vol.% H_2O to simulate a reformate off-gas after the WGS unit. The O_2 concentration was varied between 0.5 and 3 vol.% to study the effect of the O_2/CO molar ratio and N_2 was included as balance. GHSV in the 10 000–50 000

h^{-1} (STP) range have been considered for the reformate stream. These values are equivalent to feed each microchannel and microslit with 1.6–8.2 and 19.5–97.5 cm^3/min (STP) of reformate, respectively. Under these conditions, typical Knudsen numbers are well below 0.001 thus assuring the validity of the continuum model [18-20].

Catalytic reactions were modeled considering the microchannels walls as sources of products and sinks of reactants [18,19]. A reaction scheme including the oxidation of CO to CO_2, the oxidation of H_2 to H_2O and the r-WGS reaction has been considered. The kinetic equations of these reactions over the CeCu and Au/CeFe catalysts derived from the kinetic analysis were implemented in the code. CFD calculations including chemical kinetics are very demanding from the point of view of computer time. That is the reason why a first series of simulations were performed under isothermal conditions to study the effect of the main operating variables (GHSV, catalyst loading and O_2/CO molar ratio) and thus, identify the temperature windows for optimal CO removal. In a second series of simulations cooling with air was considered to investigate the capacity of microchannels and microslits with the CeCu and Au/CeFe catalysts to carry out the CO-PrOx reaction under suitable conditions.

4. Results and discussion

4.1. Kinetic analysis

The integral method of kinetic analysis was applied due to the high activity of the catalysts and wide range of the experimental variables considered that made very difficult to obtain experimental CO conversions under differential conditions. The experimental micro packed-bed reactor has been assumed to be isothermal plug-flow. As mentioned before, the absence of external diffusion limitations has been verified experimentally. The CO and O_2 conversions and selectivity data were fitted to the selected kinetic models using the Nelder

and Mead [22] algorithm of direct search furnished by the DBCPOL optimization subroutine in the IMSL library.

Initially simple power-law rate equations were adopted for the several reactions. Despite being useful in some cases, this approach failed to describe the effects of the CO_2 concentration as well as that of oxygen for the CeCu catalyst. It has been found that for a better description of the system the rate expressions of the CO consumption should include adsorption terms as given by Eqs. 1 and 2 for the CeCu and Au/CeFe catalysts, respectively:

$$-R_{CO,CeCu} = \frac{k_{CO} \cdot P_{CO} \cdot P_{O_2}^{0.5}}{\left(1 + K_{CO} \cdot P_{CO} + K_{CO_2} \cdot P_{CO_2} + K_{O_2} \cdot P_{O_2}^{0.5}\right)^2} \quad (1)$$

$$-R_{CO,Au/CeFe} = \frac{k_{CO} \cdot P_{CO} \cdot P_{O_2}^{0.5}}{1 + K_{CO} \cdot P_{CO} + K_{CO_2} \cdot P_{CO_2}} \quad (2)$$

Regarding the H_2 oxidation (Eq. 3) and reverse water-gas shift (Eq. 4) the kinetic expressions adopted the same form for both catalysts:

$$-R_{H_2} = k_{H_2} \cdot P_{H_2} \cdot P_{O_2}^{0.5} \quad (3)$$

$$-R_{rWGS} = k_{rWGS} \cdot \left(P_{H_2} \cdot P_{CO_2} - K_{WGS} \cdot P_{CO} \cdot P_{H_2O}\right) \quad (4)$$

where k_{CO}, k_{H_2} and k_{rWGS} are kinetic constants, P_i (i = CO, O_2, H_2, CO_2, H_2O) partial pressures, K_j (j = CO, O_2, CO_2,) adsorption equilibrium constants and K_{WGS} the equilibrium constant of the water-gas shift reaction. The estimated parameters are compiled in Table 1.

The conversion of CO and the O_2 selectivity to CO_2 for the CO-PrOx reaction over the two catalysts without CO_2 or H_2O in the feed are shown in Figs. 2 and 3. In these graphs points are the experimental data that have been used in the kinetic analysis and dashed lines the kinetic model fit. Fig. 2 shows the effect of varying the CO concentration for a feed with 1 vol.% O_2, whereas Fig. 3 shows the results with different O_2 concentrations for a feed containing 2 vol.% CO; in both cases the H_2 concentration in the feed was 50 vol.% and N_2

was used as balance. It can be seen that the model describes reasonably well the experimental data. It is also clear the very different performance of both catalysts. The supported gold catalyst is extremely active since CO light-off takes place below 50ºC (Fig. 2B) whereas temperatures above 150 ºC are required to achieve high CO conversions with the CeCu sample (Fig. 2A). In contrast, this solid is more selective to CO_2 irrespective of the O_2/CO ratio. This behaviour is in general accordance with previous reports in the literature [23,24]. In both cases the selectivity decreases with the reaction temperature which is due to the fact that the activation energy of the H_2 oxidation is significantly higher than that of CO oxidation (see Table 1). This is particularly true for the CeCu catalyst since in this case the activation energy of the oxidation of H_2 is very high (110 kJ/mol) which is the reason of the very good selectivity of this catalyst at low temperatures. Regarding the gold catalyst, the difference between the apparent activation energies is low, 50.0 kJ/mol for CO and 66.9 kJ/mol for H_2, which explains the smooth dependence of the selectivity on temperature in comparison with the CeCu catalyst. For these catalysts, the selectivity decreases as the O_2/CO ratio increases due to the increase of the oxygen excess. This can be seen in Figs. 2C and 2D comparing results at decreasing CO concentration and in Figs. 3C and 3D for reactions at constant CO content in the feed and increasing O_2 concentration.

Despite the huge literature existing on CO-PrOx, kinetic studies are relatively scarce, particularly those as the one in this work that takes into account simultaneously three reactions (CO and H_2 oxidation and r-WGS). Ouyang and Besser [8] have recently emphasized the importance of considering the coupling between these reactions for an accurate description of the CO-PrOx process. This of course complicates the comparison of the estimated kinetic parameters with those reported in the literature. This comparison is also complicated by the strong influence of the specific composition and preparation conditions on the performance of these catalytic systems. In the case of the CuO/CeO_2 system there is

kinetic evidence [25] on the participation of redox steps (Ce^{4+}/Ce^{3+} and Cu^{2+}/Cu^{+}) that in principle suggests the use of the Mars-van Krevelen kinetic expression. Actually, this is the approach followed by several authors although it has been found that some Langmuir-Hinshelwood (LH) models also returned satisfactorily the experimental data [26-29]. Sedmak et al. obtained apparent activation energy for the CO oxidation over a nanostructured $Cu_{0.1}Ce_{0.9}O_{2-y}$ oxide of 57.2 kJ/mol, although the H_2 oxidation and r-WGS reactions were not considered [28]. Eq. 1 in this work was previously proposed by Caputo et al. [29] who determined a surprisingly high apparent activation energy of 205 kJ/mol for CO oxidation over a 4 wt.% CuO/CeO_2 catalyst. Our estimated value of 36.9 kJ/mol is more in line with some results by Liu and Flytzani-Stephanopoulos [26,27] for low copper-containing $Cu\text{-}CeO_2$ catalysts, and is very close to the value measured by Jernigan and Somorjai over metallic copper (37.6 kJ/mol) [30]. Regarding gold catalysts it is well known that the best supports for this metal are those that are also active for CO oxidation such as $\alpha\text{-}Fe_2O_3$ [31] and nanocrystalline ceria [32] that supply reactive oxygen species to the surface of the gold particles. The value of the apparent activation energy for CO oxidation over Au/CeFe estimated in this work (50.0 kJ/mol) is close to the 54 kJ/mol found by Aguilar-Guerrero and Gates [33] for CO oxidation over small clusters (9 Å) of gold dispersed over CeO_2. Slightly lower values (46 kJ/mol) were measured by Schubert et al. [34] in the presence of CO_2 and water over Au/ $\alpha\text{-}Fe_2O_3$ so it can be concluded that the performance of gold supported on these two oxides is similar. As shown in Table 1, the adsorption heat of CO on Au/ $\alpha\text{-}Fe_2O_3$ is very low (6.7 kJ/mol) which is a well-known feature of this system [31] and contributes to the loss of selectivity to CO_2 on increasing the temperature. The strength of CO adsorption on CeCu is higher with a heat of adsorption of 11 kJ/mol, in accordance with the literature [27]; this also contributes to the superior selectivity of this solid compared with Au/CeFe.

4.2. Effects of the presence of CO_2 and water in the feed

The effect of the presence of CO_2 and H_2O in the feed is a critical issue of CO-PrOx for fuel cell applications since the reformate off-gas typically contains high concentrations of these compounds. The conversion of CO for the CO-PrOx reaction over the CeCu and Au/CeFe catalysts with CO_2 and H_2O in the feed is shown in Fig. 4. Figs. 4A and 4B show the effect of changing the CO_2 concentration in a dry feed, whereas in Figs. 4C and 4D the results are for experiments with a feed containing 2 vol.% CO_2 and different water concentrations; in all cases the concentration of H_2 in the feed was 50 vol.%, that of CO and O_2 1 vol.% and N_2 was used as balance. It can be seen that the model also describes reasonably well the experimental data obtained with CO_2 and H_2O in the feed.

The presence of CO_2 in the feed has a negative effect on the catalytic activity which is especially strong for the CeCu oxide. This is reflected in the kinetic model by large values of the heat of CO_2 adsorption which amount to 79.8 kJ/mol over CeCu and 26 kJ/mol over Au/CeFe (Table 1). However, this effect is much less pronounced when the temperature increases as it is apparent in Figs. 4A and 4B. Moreover, the selectivity remains almost unchanged (results not shown) in the presence of CO_2 thus meaning that the inhibiting effect is equivalent on both CO and H_2 oxidation reactions as found in previous works [23,29]. These evidences point to competitive adsorption of CO_2 over the CeCu catalyst as the cause of this effect [29]. It has been also proposed that CO_2 hinders the redox processes by stabilizing oxidized copper species [35]. In contrast, this solid is tolerant to the presence of water vapour. In fact, as shown in Fig. 4C the CO conversion is not significantly affected by H_2O concentrations in the feed up to 20 vol.%; the selectivity does not change either. This is a very interesting result taking into account that it is usually found that H_2O is a much stronger inhibitor than CO_2 for the reaction of CO oxidation over this catalytic system [36]. Good resistance to water was also found by Liu and Flytzani-Stephanopoulos for Cu-Ce, Co-Ce and

Cu-Zr fluorite oxide composite catalysts [37]. Regarding supported gold catalysts, the inhibiting effect of CO_2 is attributed to carbonate ($FeCO_3$) formation that lowers the electron density of CO and blocks anionic sites on the support where oxygen adsorption takes place. As discussed by Bond et al. [31], in this case the presence of water has a beneficial effect since carbonate formation is inhibited and the selectivity to CO_2 increases due the tendency of H_2O to preferentially suppress H_2 oxidation. Our results are in accordance with this interpretation since the CO conversion increases with the water vapour concentration (Fig. 4D) and the selectivity to CO_2 also increases slightly.

4.3. Isothermal CFD simulations: Effects of the operating variables and the aspect ratio

The kinetic model established by Eqs. 1-4 and the parameters compiled in Table 1 have been implemented in CFD codes to simulate the CO-PrOx reaction in microchannels and microslits as described in section 3 for a feed containing 70 vol.% H_2, 1 vol.% CO, 10 vol.% CO_2 and 10 vol.% H_2O. A first series of simulations under isothermal conditions were carried out to study the effect of some of the main operating variables; the results are included in Fig. 5. Fig. 5A shows the mean CO content at the microchannels outlet as a function of the reaction temperature and catalyst loading at GHSV of 10 000 h^{-1} and O_2/CO molar ratio of 2. As evidenced with the kinetic study the performance of the two catalysts considered in this work is very different. It can be seen that with the gold catalyst the CO content at the reactor outlet decreases at decreasing temperatures; however, even with a high catalyst loading of 5 mg/cm^2 it is difficult to lower the CO concentration below 100 ppmv due to the limited selectivity of the Au/CeFe solid. In the case of the CeCu catalyst, on the other hand, it is possible to achieve very low CO exit concentrations in the 1-10 ppmv range with catalyst loadings between 1 and 5 mg/cm^2. An optimum temperature exists at which the CO concentration at the microchannel outlet is minimal. Under the conditions of the simulations

presented in Fig. 5A, this temperature increases from 172 ºC for 5 mg/cm^2 to 190 ºC for 2 mg/cm^2 and 200 ºC for 1 mg/cm^2. This optimum is the result of the opposite effect of temperature on the CO conversion and O_2 selectivity to CO_2 (see Figs. 2A and 2B). Interestingly, the minimal CO content coincides with values of the O_2 conversion close to 100%.

The effect of the GHSV is shown in Fig. 5B for a catalyst loading of 5 mg/cm^2 and O_2/CO molar ratio of 2. Conclusions similar to those obtained for the effect of the catalyst loading can be drawn. With the supported gold catalyst obtaining CO outlet concentrations below 100 ppmv is only possible at low space velocities (GHSV < 10 000 h^{-1}) and temperatures if the amount of catalyst is high enough. In the case of the CeCu catalyst it is possible to obtain very low CO contents at the microchannels outlet working at an optimal temperature that increases with the space velocity. This temperature can reach 200 ºC for the very high GHSV of 50 000 h^{-1}. The effect of the O_2/CO molar ratio is shown Fig. 5C for a catalyst loading of 1 mg/cm^2 and GHSV of 10 000 h^{-1}. In this case the existence of an optimum operating temperature with the Au/CeFe catalyst is more clearly seen since it is displaced to higher temperatures compared with the conditions of the previous simulations. Nevertheless, although the minimal CO content decreases with increasing the O_2/CO ratio its value is above 500 ppmv which is too high as to have practical interest. In the case of the CeCu catalyst, on the other hand, even with the relatively low catalyst loading of 1 mg/cm^2, the use of O_2/CO ratio of 2 or above allows obtaining below 50 ppmv of CO at the microreactor outlet. Unfortunately, under these conditions the O_2 selectivity to CO_2 is low, resulting in H_2 conversions between 4.4 and 7.8 % that, although being significant, might be admissible in certain circumstances.

Simulations have been also conducted to examine possible effects between the performance of the microchannels and microslits while keeping up the characteristic

dimension of both geometries in 0.7 mm. To take into account the different wall surface area-to-volume ratio comparisons have been made at the same weight-hourly space velocity (WHSV) of 83, 149 and 415 h^{-1}. To get an idea the last value corresponds to GHSV of 50 000 h^{-1} and 596 430 h^{-1} for the microchannels and microslits, respectively. The catalyst loading was 1 mg/cm^2 and the O_2/CO molar ratio 2. As can be seen in Figs. 6A and 6B the performance of both geometries is almost coincident. An inspection of the CFD results has evidenced the absence of concentration profiles along the characteristic dimension in both cases which explains the equivalent performance of the microchannels and microslits provided the characteristic dimension is kept constant. It should be noted that microslits are much easier to fabricate than microchannels; therefore, the lower fabrication costs may be an interesting advantage in favour of microslits in this case.

4.4. Control of the CO-PrOx temperature

Isothermal simulations showed up that there is an optimum operating temperature at which the CO content at the reactor outlet is minimized. In this section, the potential of microreactors to work close to the ideal conditions by coupling the exothermal CO-PrOx reaction with cooling by air is examined. This part of the study has been performed with the CeCu catalyst since it is the only theoretically capable of achieving under optimal conditions CO content reductions of practical interest for PEMFC applications.

This approach to control the CO-PrOx temperature is interesting from the point of view of the system integration as shown by Delsman et al. [38]. These authors studied experimentally and by model simulation a microdevice consisting of a preferential oxidation-heat exchanger unit constructed from microstructured stainless-steel plates and sized to feed a 100 W_e fuel cell. In this device, the combined fuel cell anode and cathode exhaust gas, mainly consisting of air with about 5% H_2, is preheated up to about 110 ºC with the CO-free

reformate and fed into the cooling plates of the CO-PrOx reactor in counter-current arrangement. After exiting the reactor at about 175 ºC it is sent to another heat exchange zone where it is heated with the hot reformate stream and finally fed into a catalytic burner to provide heat for the fuel (methanol/water) vaporizer and reformer. In other studies, oil [11], air in co-current arrangement [39], and water vaporization [9,10] have been adopted for cooling purposes.

In this work, non-isothermal CFD simulations have been conducted for a feed stream containing 70 vol.% H_2, 1 vol.% CO, 2 vol. % O_2, 10 vol.% CO_2, 10 vol.% H_2O and 7 vol.% N_2 entering the reaction channels at 200 ºC with GHSV of 18 000 h^{-1}. A catalyst (CeCu) loading of 5 mg/cm^2 has been considered. For this case, the optimal temperature is about 184 ºC (see Fig. 5B). Cooling is performed with co-current air in neighbouring channels or slits. The effect of the air inlet temperature (80, 120 or 150 ºC) and flow rate on the mean temperature and CO content at the reactor outlet is shown in Figs. 7A and 7B, respectively. It can be seen that for each inlet temperature there is a flow rate (expressed as the ratio between the mass flow rates of the air and CO-PrOx streams) that allows obtaining an exit temperature close to the desired value. Obviously, this flow rate has to increase with the inlet air temperature. However, when using relatively low air temperatures (80 ºC) there is the risk that if a small uncontrolled increase of the air flow rate takes place the CO-PrOx reaction can extinguish resulting in a sudden increase of the CO content in the off-gas. For this reason it is recommendable to use air at a temperature not too far from the optimal value; for example, between 120 and 150 ºC for the conditions considered in this section. This has the disadvantage of requiring high air flow rates, between 30 and 60 times that of the reformate stream. Another option could be using water saturated at a suitable pressure as previously proposed for the Fischer-Tropsch synthesis in microreactors [20]; however, this would be an

unnecessary complication in the case of the CO-PrOx process that can be advantageously operated at atmospheric pressure.

In this case there is again no difference between using microchannels or microslits with the same characteristic dimension. Fig. 8 shows the evolution of the CO concentration and temperature in a central plane along these geometries (total length of 20 mm) for a case with air inlet temperature of 120 ºC and ratio between the mass flow rates of the cooling air and PrOx streams of 26. It can be seen that the CO content decreases rapidly to reach a minimum value close to 1 ppmv at about 11 and 14 mm from the entry in the microchannels and microslits, respectively. Then, there is a slight increase of the CO content that can be attributed to the r-WGS reaction and finally the stream exits the reactor with a CO content of 3-4 ppmv. As concerns the temperature, it changes very quickly, especially in the microchannels, as expected from the increased heat transfer rate due to their higher surface area-to-volume ratio. Nervertheless, for the two geometries, the air and PrOx temperatures become the same at half length (10 mm), almost coinciding with the minimum of CO concentration, which evidences the very efficient heat transfer performance of these devices. As shown in Fig. 8C the temperature in the solid domain is very uniform and close to the value at which the fluids exit from the microreactor.

4. Conclusions

Microreaction technology can respond to the demanding challenges posed by some chemical reactions. This is the case of the CO-PrOx process that is very exothermic and is characterized by a complex scheme of competing reactions in which heat transfer issues reach great relevance. A careful control of the reaction temperature is required in order to attain suitable oxygen selectivity to CO_2. Moreover, an active catalyst is needed to reduce the CO

content of the hydrogen-rich stream to the trace-level required for low-temperature PEM fuel cells operation. The kinetic study performed in this work has shown that a properly prepared cerium-copper oxide catalyst fulfils the activity and selectivity requirements of the CO-PrOx process even though CO_2 and H_2O are present in the reformate stream. CFD simulations have evidenced that due to the opposite effect of temperature on activity and selectivity there is an optimal temperature at which the CO content over the CeCu catalyst can reach values well below 100 ppmv and even 10 ppmv under suitable conditions such as relatively high catalyst loadings (2-5 mg/cm^2) and O_2/CO ratios (2 or above). Control of the reaction temperature is possible in reactors based on microchannels and microslits owing to the excellent heat transfer characteristics of these devices. The performance of both geometries is very similar provided the characteristic dimension is kept constant.

Acknowledgements

We gratefully acknowledge financial support of this work by the Spanish Ministry of Science and Innovation (MAT2006-12386-C05 and ENE2009-14522-C04).

References

[1] J.D. Holladay, J. Hu, D.L. King, Y. Wang, Catal. Today 139 (2009) 244.

[2] G. Kolb, V. Hessel, V. Cominos, C. Hofmann, Hl Löwe, G. Nikolaidis, R. Zapf, A. Ziogas, E.R. Delsman, M.H.J.M. de Croon, J.C. Schouten, O. de la Iglesia, R. Mallada, J. Santamaria, Catal. Today 120 (2007) 2.

[3] E.D. Park, D. Lee, H.C. Lee, Catal. Today 139 (2009) 280.

[4] A. Gavriilidis, P. Angeli, E. Cao, K.K. Yeong, Y.S.S. Wan, Chem. Eng. Res. Des. 80 (2002) 3.

[5] G. Kolb, V. Hessel, Chem. Eng. J. 98 (2004) 1.

[6] X. Ouyang, L. Bednarova, P. Ho, R.S. Besser, AIChE J. 51 (2005) 1758.

[7] X. Ouyang, R.S. Besser, J. Power Sources 141 (2005) 39.

[8] X. Ouyang, R.S. Besser, CO Clean-up: Preferential Oxidation, in: V. Hessel, A. Renken, J.C. Schouten and J.-I. Yoshida (Eds.), Micro Process Engineering, Vol. 2: Devices, Reactions and Applications, Wiley-VCH Verlag, Weinheim, 2009, p. 479.

[9] G. Kolb, C. Hofmann, M. O'Connell, J. Schürer, Catal. Today 147S (2009) S176.

[10] M. O'Connell, G. Kolb, K.-P. Schelhaas, J. Schuerer, D. Tiemann, A. Ziogas, V. Hessel, Int. J. Hydrogen Energy 35 (2010) 2317.

[11] C.D. Dudfield, R. Chen, P.L. Adcock, J. Power Sources 86 (2000) 214.

[12] C.D. Dudfield, R. Chen, P.L. Adcock, Int. J. Hydrogen Energy 26 (2001) 763.

[13] V. Cominos, V. Hessel, C. Hofmann, G. Kolb, R. Zapf, A. Ziogas, E.R. Delsman, J.C. Schouten, Catal. Today 110 (2005) 140.

[14] S.-M. Hwang, O.J. Kwon, S.H. Ahn, J.J. Kim, Chem. Eng. J. 149 (2009) 105.

[15] P.V. Snytnikov, M.M. Popova, Y. Men, E.V. Rebrov, G. Kolb, V. Hessel, J.C. Schouten, V.A. Sobyanin, Appl. Catal. A: Gen. 350 (2008) 53.

[16] H. Provendier, C. Petit, J.L. Schmitt, A. Kiennemann, C. Chaumont, J. Mater. Sci. 34 (1999) 4121.

[17] T. Glatzel, C. Litterst, C. Cupelli, T. Lindermann, C. Moosmann, R. Niekrawietz, W. Streule, R. Zengerle, P. Koltay, Comput. Fluids 37 (2008) 218.

[18] G. Arzamendi, P.M. Diéguez, M. Montes, M.A. Centeno, J.A. Odriozola, L.M. Gandía, Catal. Today 143 (2009) 25.

[19] G. Arzamendi, P.M. Diéguez, M. Montes, J.A. Odriozola, E. Falabella Sousa-Aguiar, L.M. Gandía, Chem. Eng. J. 154 (2009) 168.

[20] G. Arzamendi, P.M. Diéguez, M. Montes, J.A. Odriozola, E. Falabella Sousa-Aguiar, L.M. Gandía, Chem. Eng. J. 160 (2010) 915.

[21] J. Blazek, Computational Fluid Dynamics: Principles and Applications, Elsevier, Amsterdam, 2005.

[22] J.A. Nelder, R.A. Mead, Comput. J. 7 (1965) 308.

[23] G. Avgouropoulos, T. Ioannides, H.K. Matralis, J. Batista, S. Hocevar, Catal. Lett. 73 (2001) 33.

[24] G. Avgouropoulos, T. Ioannides, Ch. Papadopoulou, J. Batista, S. Hocevar, H.K. Matralis, Catal. Today 75 (2002) 157.

[25] M. Moreno, L. Bergamini, G.T. Baronetti, M.A. Laborde, F.J. Mariño, Int. J. Hydrogen Energy 35 (2010) 5918.

[26] W. Liu, M. Flytzani-Stephanopoulos, Chem. Eng. J. 64 (1996) 283.

[27] W. Liu, M. Flytzani-Stephanopoulos, J. Catal. 153 (1995) 317.

[28] G. Sedmak, S. Hočevar, J. Levec, J. Catal. 213 (2003) 135.

[29] T. Caputo, L. Lisi, R. Pirone, G. Russo, Ind. Eng. Chem. Res. 46 (2007) 6793.

[30] G.G. Jernigan, G.A. Somorjai, J. Catal. 147 (1994) 567.

[31] G.C. Bond, C. Louis, D.T. Thompson, Catalysis by Gold, in: G.J. Hutchings (Ed.) Catalytic Science Series, Vol. 6, Imperial College Press, London, 2006, p. 210.

[32] J. Guzman, S. Carrettin, A. Corma, J. Am. Chem. Soc. 127 (2005) 3286.

[33] V. Aguilar-Guerrero, B.C. Gates, J. Catal. 260 (2008) 351.

[34] M.K. Schubert, A. Venugopal, M.J. Kahlich, V. Plzak, R.J. Behm, J. Catal. 222 (2004) 32.

[35] D.H. Kim, J.E. Cha, Catal. Lett. 86 (2003) 107.

[36] G. Avgouropoulos, T. Ioannides, Appl. Catal. B: Environ. 67 (2006) 1.

[37] W. Liu, M. Flytzani-Stephanopoulos, J. Catal. 153 (1995) 304.

[38] E.R. Delsman, M.H.J.M. de Croon, A. Pierik, G.J. Kramer, P.D. Cobden, Ch. Hofmann, V. Cominos, J.C. Schouten, Chem. Eng. Sci. 59 (2004) 4795.

[39] F. Cipitì, V. Recupero, Chem. Eng. J. 146 (2009) 128.

Captions

Table 1 Estimated kinetic parameters of the rate equations for the catalysts indicated.

Fig. 1 Meshes applied to the fluidic and solid domains of the microchannel (A) and microslit (B) geometries.

Fig. 2 Effect of the CO concentration on the CO conversion and O_2 selectivity to CO_2 of the CeCu (A,C) and Au/CeFe (B,D) catalysts without CO_2 or H_2O in the feed. Space-time: 1 ($g_{cat.}$·min)/l. Points are experimental data and dashed lines the kinetic model fit.

Fig. 3 Effect of the O_2 concentration on the CO conversion and O_2 selectivity to CO_2 of the CeCu (A,C) and Au/CeFe (B,D) catalysts without CO_2 or H_2O in the feed. Space-time: 1 ($g_{cat.}$·min)/l. Points are experimental data and dashed lines the kinetic model fit.

Fig. 4 Effect of the CO_2 and H_2O concentration on the CO conversion of the CeCu (A,C) and Au/CeFe (B,D) catalysts. Space-time: 1 ($g_{cat.}$·min)/l. Points are experimental data and dashed lines the kinetic model fit.

Fig. 5 Effect of the catalyst loading (A), GHSV (B) and O_2/CO molar ratio (C) on the mean CO concentration at the microchannel outlet according to isothermal CFD simulations with the CeCu and Au/CeFe catalysts under the conditions indicated.

Fig. 6 Comparison between the performance of microchannels (solid symbols) and microslits (open symbols) with the CeCu (A) and Au/CeFe (B) catalysts according to isothermal CFD simulations under the conditions indicated.

Fig. 7 Effect of the air flow rate and inlet temperature on the mean temperature (A) and CO content (B) at the microchannels outlet according to CFD simulations with the CeCu catalyst for a CO-PrOx feed stream at 200 ºC with GHSV of 18 000 h^{-1}.

Fig. 8 Evolution of the CO content (A,B) and temperature (A,C) in a central plane along a microchannel (solid line) and microslit (dashed line) using air at 120 ºC and a ratio between the mass flow rates of the cooling air and PrOx streams of 26.

Table 1. Estimated kinetic parameters of the rate equations for the catalysts indicated. [a]

Parameter	CeCu	Au/CeFe
k_{CO} [mol/(s·$g_{cat.}$·$atm^{1.5}$)]	4.15	0.194
$E_{A,CO}$ [kJ/mol]	36.9	50.0
K_{CO} [atm^{-1}]	8.7	48.1
$(-\Delta H)_{CO}$ [kJ/mol]	11.0	6.7
K_{CO_2} [atm^{-1}]	$1.12 \cdot 10^{3}$	26.4
$(-\Delta H)_{CO_2}$ [kJ/mol]	79.8	26.0
K_{O_2} [$atm^{-0.5}$]	219	-
$(-\Delta H)_{O_2}$ [kJ/mol]	1.7	-
k_{H_2} [mol/(s·$g_{cat.}$·$atm^{1.5}$)]	$8.9 \cdot 10^{-7}$	$1.2 \cdot 10^{-3}$
E_{A,H_2} [kJ/mol]	110	66.9
k_{rWGS}[mol/(s·$g_{cat.}$·atm^{2})]	$5 \cdot 10^{-9}$	$1.1 \cdot 10^{-6}$
$E_{A,rWGS}$ [kJ/mol]	36.9	96.6

[a] Values of the kinetic and adsorption equilibrium constants are given at 100 ºC. E_A stands for apparent activation energy and ($-\Delta H$) for heat of adsorption.

Table 1.

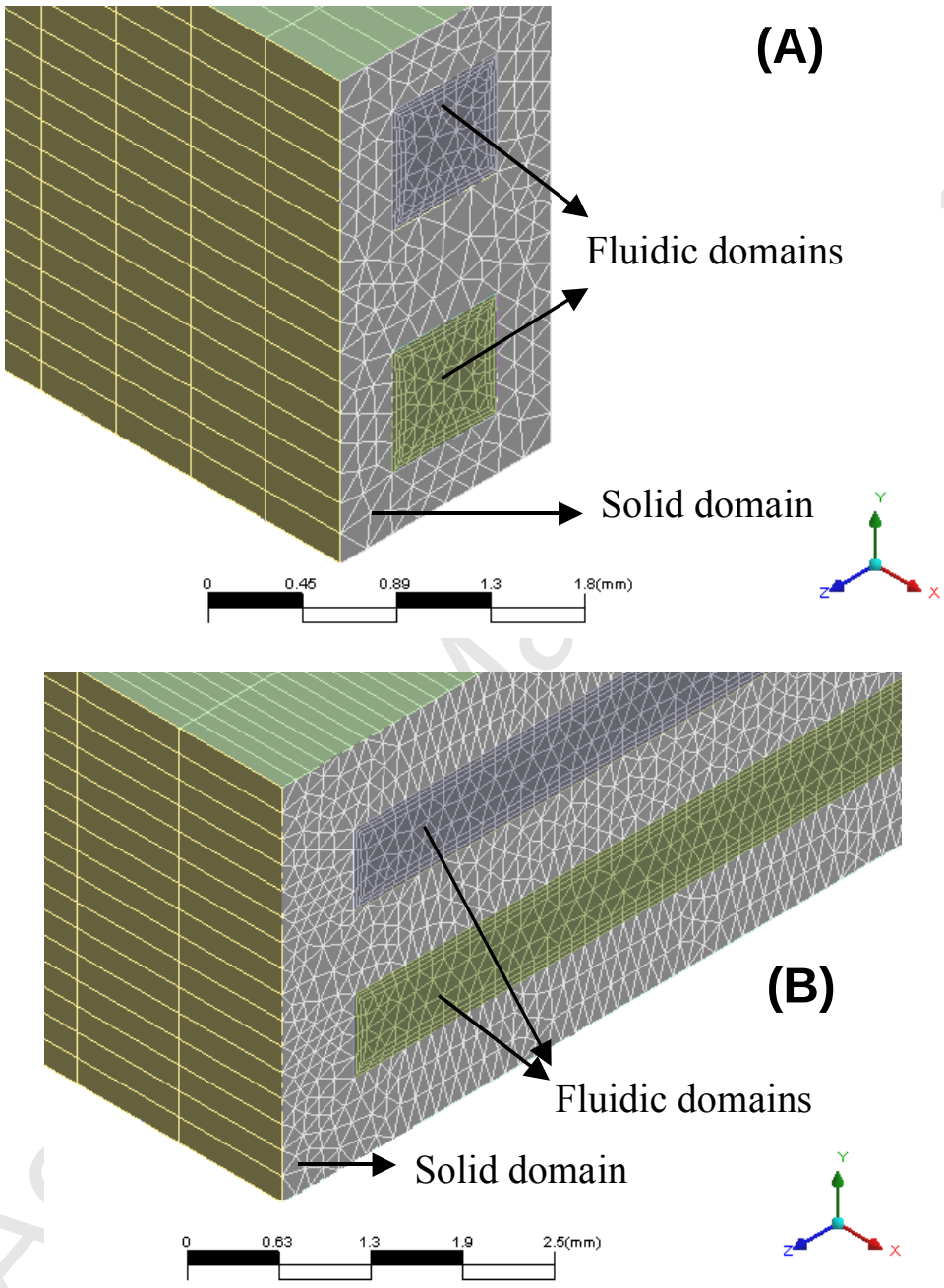

Fig. 1.

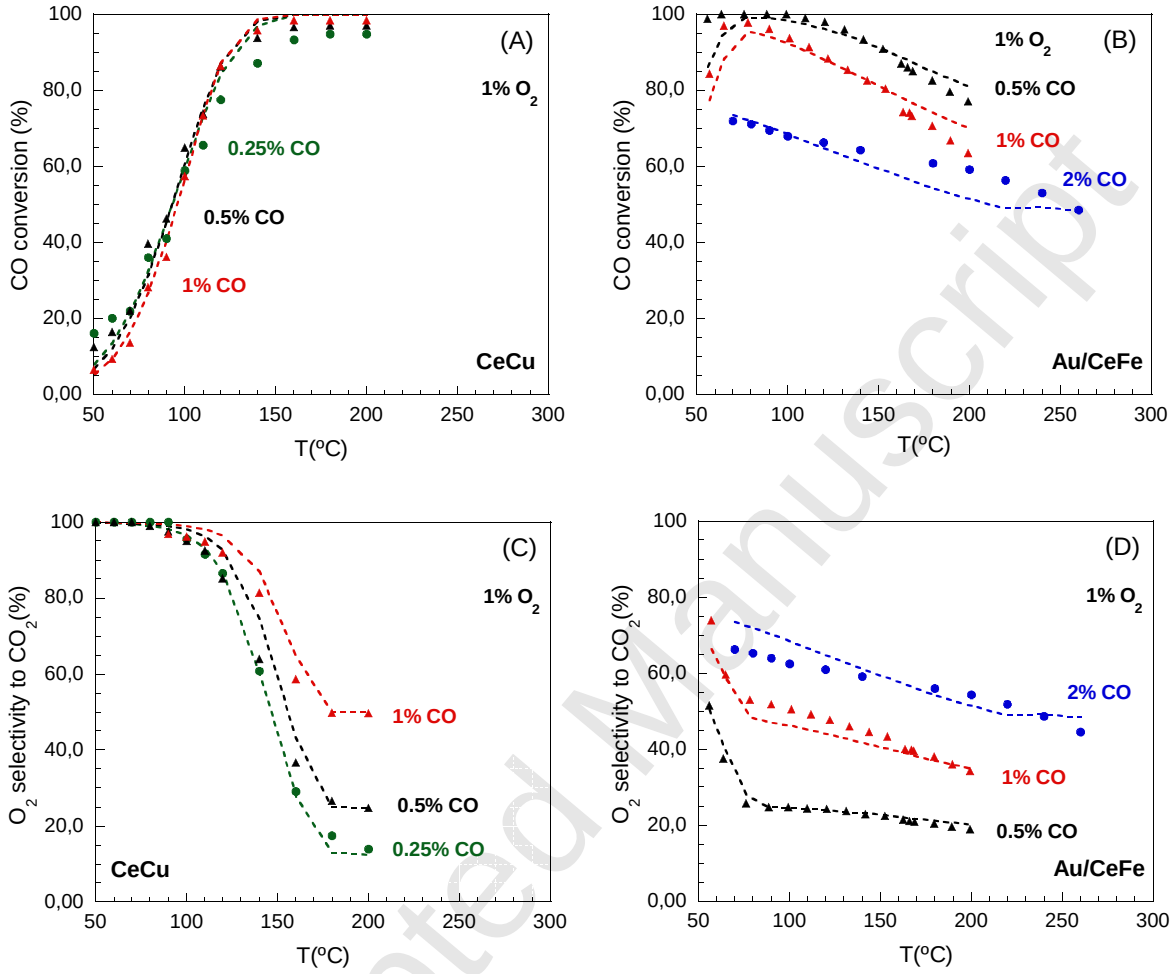

Fig. 2.

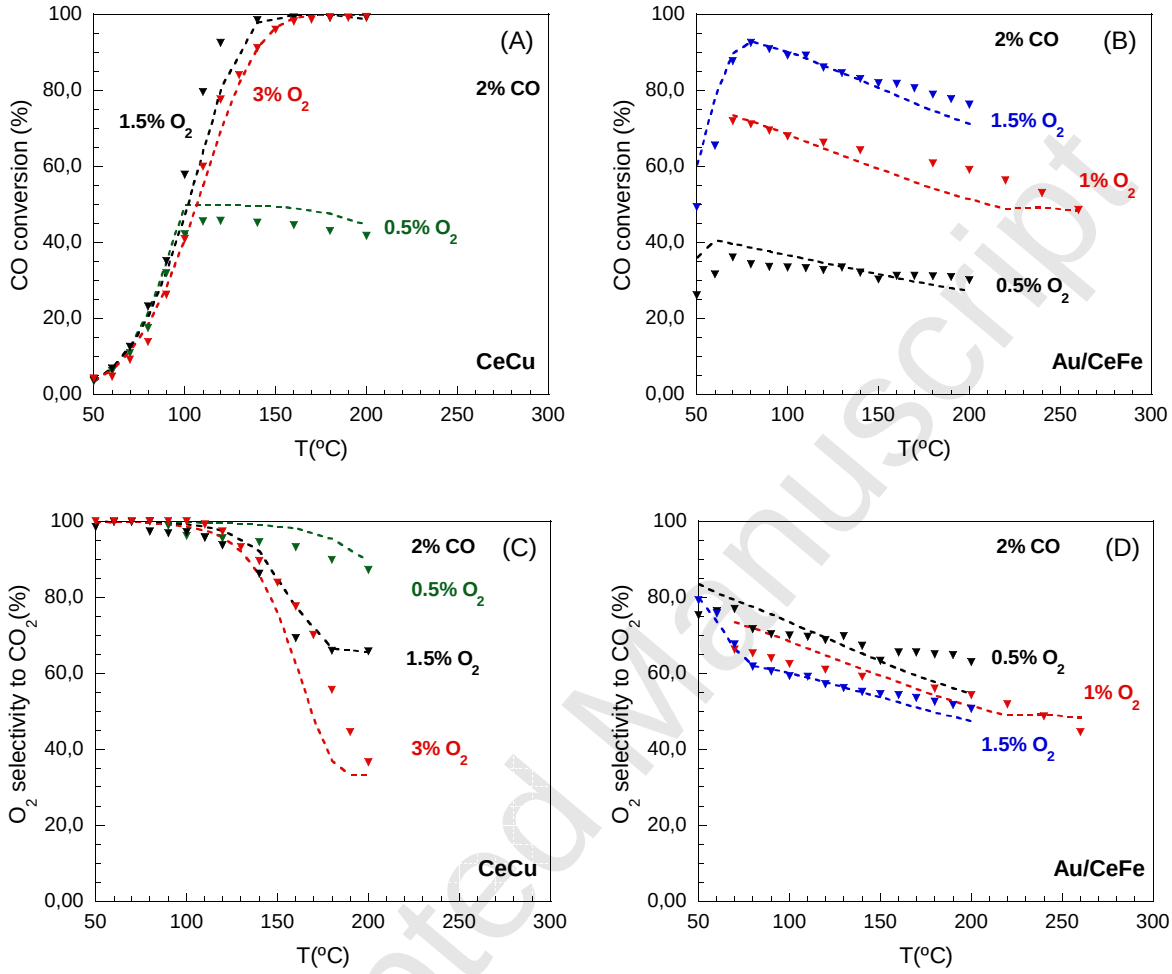

Fig. 3.

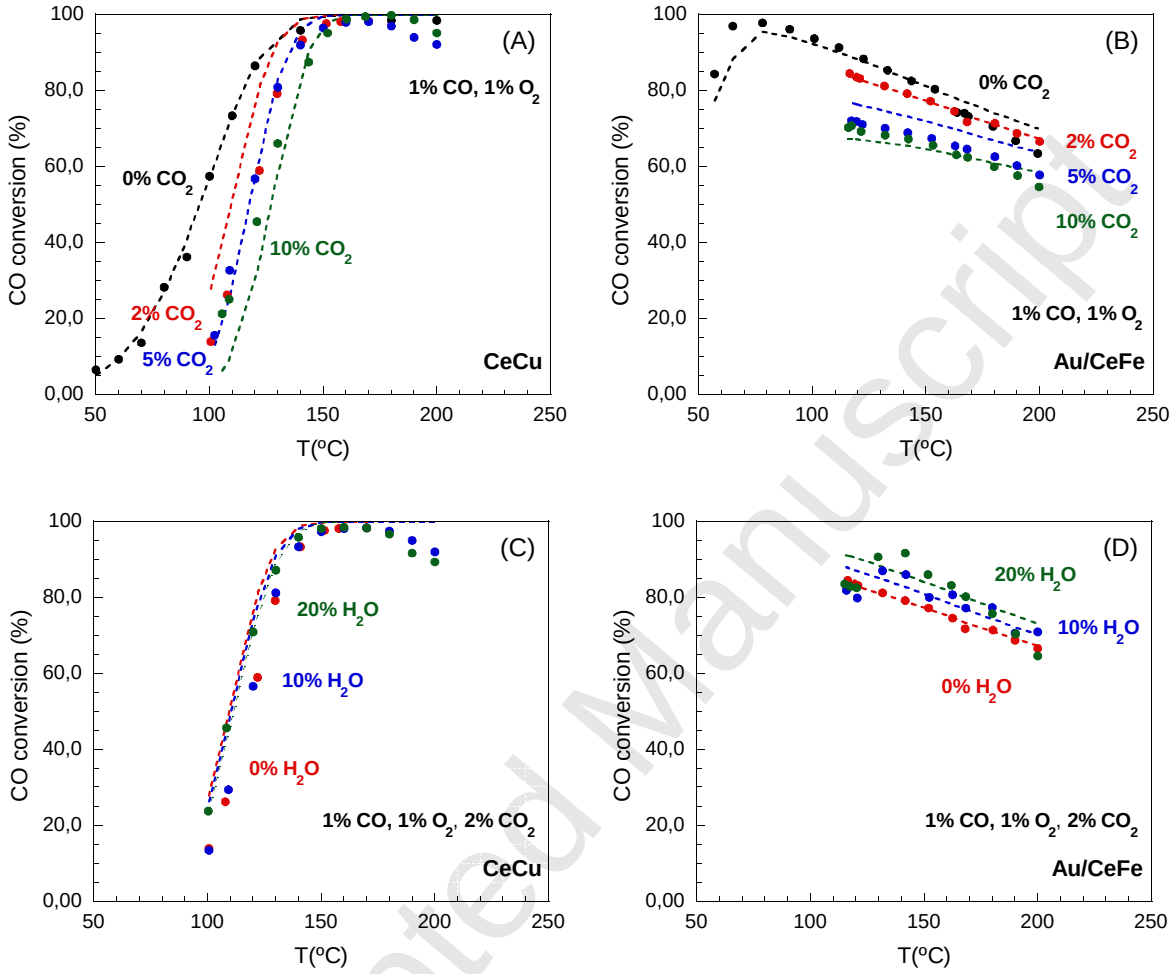

Fig. 4.

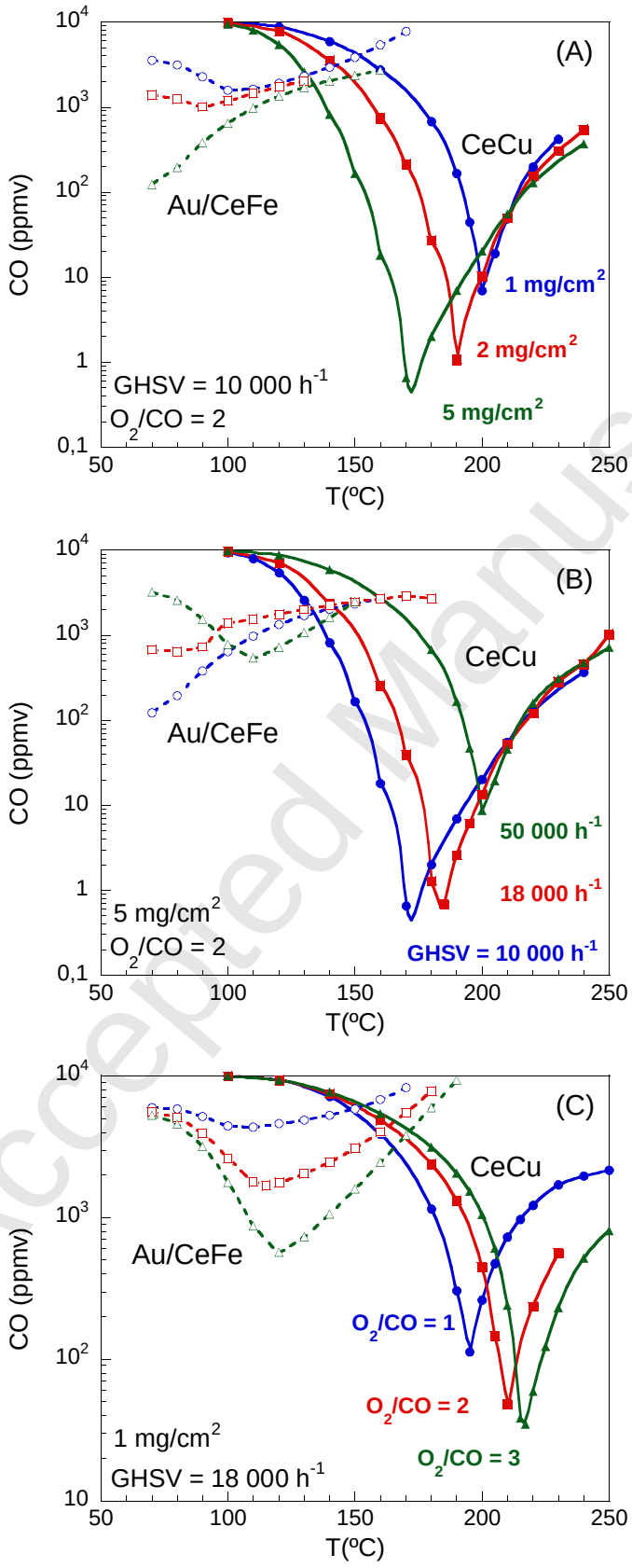

Fig. 5.

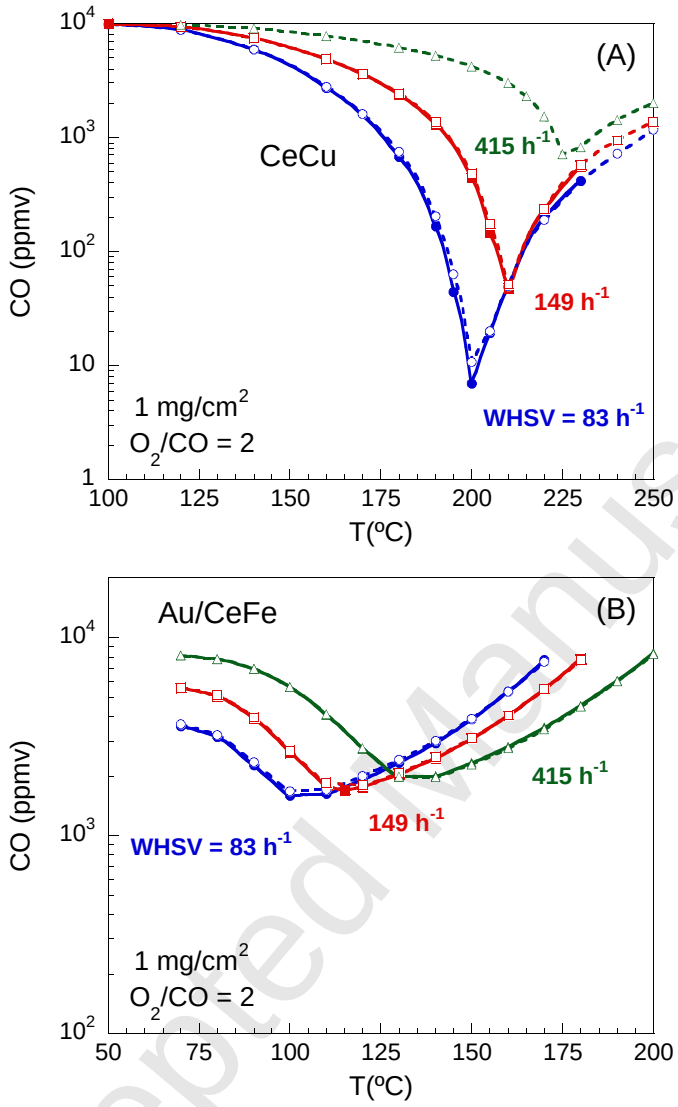

Fig. 6.

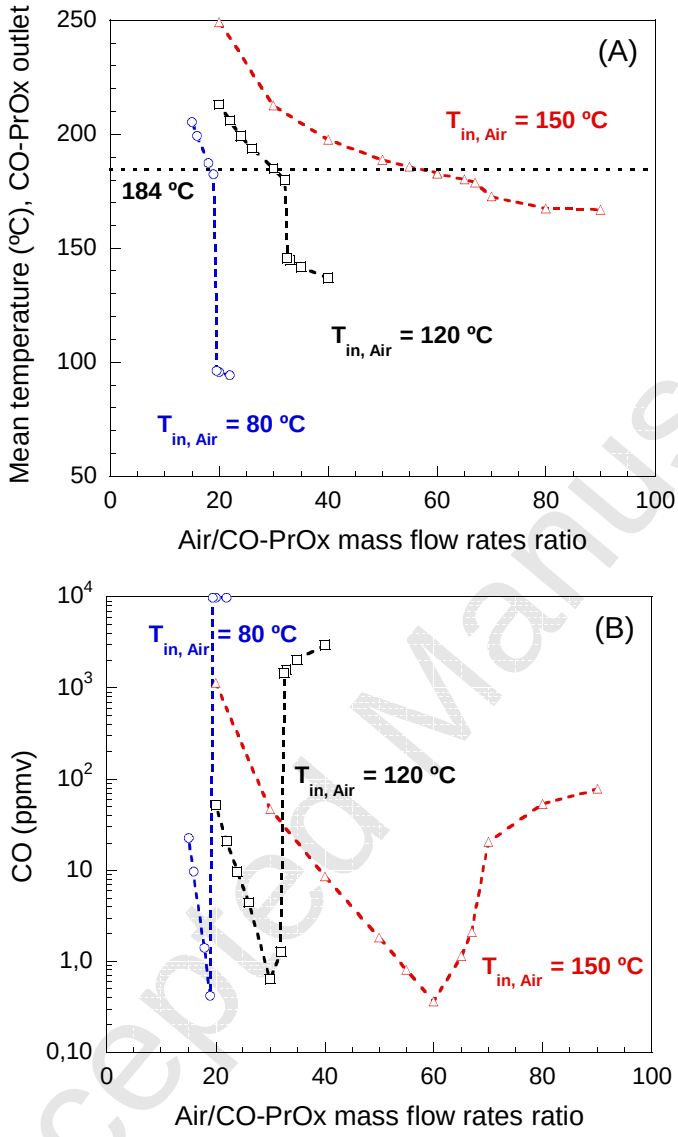

Fig. 7.

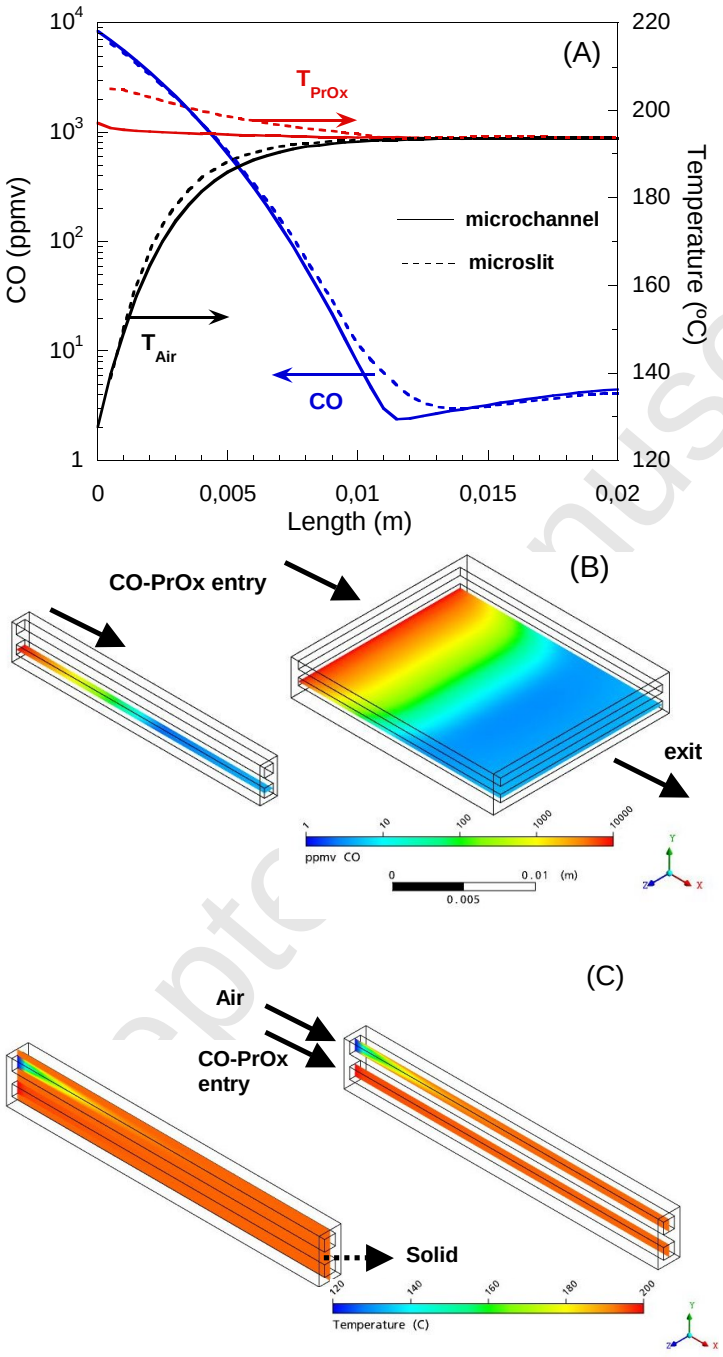

Fig. 8.